PHYSICAL REVIEW B VOLUME 62, NUMBER 8 15 AUGUST 2000-II

Current-carrying capacity of carbon nanotubes

M. P. Anantram
NASA Ames Research Center, Mail Stop T27A-1, Moffett Field, California 94035-1000
(Received 18 October 1999; revised manuscript received 12 April 2000)

The current carrying capacity of ballistic electrons in carbon nanotubes that are coupled to ideal contacts is analyzed. At small applied voltages, electrons are injected only into crossing subbands, the differential conductance is $4e^2/h$. At applied voltages larger than $\Delta E_{NC}/2e$ (ΔE_{NC} is the energy level spacing of first noncrossing subbands), electrons are injected into noncrossing subbands. The contribution of these electrons to current is determined by the competing processes of Bragg reflection and Zener-type intersubband tunneling. In small diameter nanotubes, Bragg reflection dominates, and the maximum differential conductance is comparable to $4e^2/h$. Intersubband Zener tunneling can be non-negligible as the nanotube diameter increases, because ΔE_{NC} is inversely proportional to the diameter. As a result, with increasing nanotube diameter, the differential conductance becomes larger than $4e^2/h$, though not comparable to the large number of subbands into which electrons are injected from the contacts. These results may be relevant to recent experiments in large diameter multiwall nanotubes that observed conductances larger than $4e^2/h$.

INTRODUCTION

Most experimental[1–3] and theoretical work of electron transport in individual nanotubes deals with single wall nanotubes (SWNT). In these experiments, the spacing between subbands is typically larger than the applied voltage and thermal energy kT. Recent experiments[4–6] on multiwall nanotubes (MWNT) are fundamentally different in that the subband spacing is comparable to the applied voltage and only a few times larger than the room temperature kT. It is further believed that transport in these experiments primarily takes place along individual layers, with little interlayer coupling. From the viewpoint of molecular electronics, the relatively small low bias resistance of 500 Ω in multiwall nanotube wires reported in Ref. 6 is very promising. In addition, Ref. 4 found that the increase in differential conductance with applied voltage was not commensurate with the increase in number of subbands in large diameter nanotubes. On the theoretical side, Ref. 7 found long tails in the screening properties of metallic nanotubes. Motivated by the above work, we study the ballistic current carrying capacity of electrons injected into a nanotube by including the noncrossing subbands.

CENTRAL IDEA AND BASIC PROCESSES INVOLVED

The central idea of this paper is that an applied bias across the nanotube results in a *transport bottleneck* due to Bragg reflection. This results in a smaller than expected increase in differential conductance with an increase in applied bias.

In a defect-free nanotube connected to ideal contacts, there are three possibilities for an electron injected from the left contact (Fig. 1): (i) Direct transmission, where an electron is transmitted in the injected subband (solid line of Fig. 1), (ii) Bragg reflection, which occurs when the wave vector (k) of an injected electron evolves to a value where the velocity in subband n, $v_n(k)=(1/\hbar)[dE_n(k)/dk]=0$ (subband extrema). In Fig. 1, an electron injected from the left contact into a noncrossing subband undergoes Bragg reflection at the location of the arrow (dotted line), and (iii) intersubband Zener-type tunneling, which involves tunneling between subbands induced by an electric field. The spacing between noncrossing subbands (ΔE_{NC} of Fig. 1) decreases inversely with increase in nanotube diameter (D), $\Delta E_{NC} \propto 1/D$. So, we surmise that Zener tunneling becomes more important in determining the I-V curve with an increase in nanotube diameter. The relative importance of these three phenomena depends on the energy, potential profile, and nanotube diameter, as discussed in this paper.

METHOD

The current is computed using the Landauer-Buttiker formula,

$$I=\int dE\, T(E)[f_L(E)-f_R(E)], \tag{1}$$

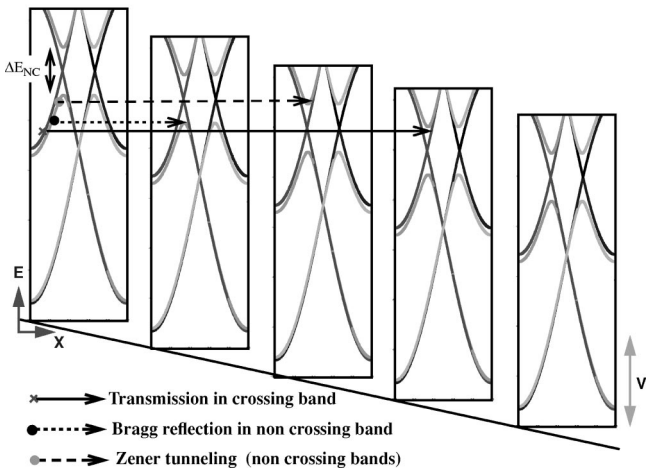

FIG. 1. Each rectangular box is a plot of energy versus wave vector, with the subband bottom equal to the electrostatic potential. Only a few subbands are shown for the sake of clarity. The three processes shown are direct transmission (solid line), Bragg reflection (dotted line), and intersubband Zener tunneling (dashed line).

where $T(E)$ is the total transmission (single particle transmission probability summed over all subbands), and $f_L(E)$ and $f_R(E)$ are the Fermi factors in the left (μ_L) and right (μ_R) contacts, respectively. We calculate the total transmission within the context of the π-orbital approximation, where the hopping parameter is assumed to be 3.1 V. The method to calculate the total transmission is the same as in Ref. 8. The calculation of the I-V curve requires the potential drop across the nanotube. The potential drop should in principle be determined by the self-consistent solution of Poisson's equation and the nonequilibrium electron density. This is a difficult problem for nanostructures. So, to convey the essential physics illustrating the role of Zener tunneling, we assume analytical profiles to simulate different values of the electric field, as discussed below. Finally, the nanotube is assumed to be coupled to ideal contacts, which means semi-infinite nanotube leads. So, a work function mismatch between the nanotube and real contacts, and the accompanying electrostatics is neglected.

RESULTS

The total transmission (and hence current) is determined by two physical parameters:

(i) ΔE_{NC}, the energy level spacing between the first noncrossing subbands (Fig. 1). ΔE_{NC} depends on diameter, and for a (N,N) nanotube,

$$\Delta E_{NC} = 2t_0 \sin\left(\frac{\pi}{N}\right), \tag{2}$$

where t_0 is the hopping parameter between nearest neighbor carbon atoms. At applied voltages smaller than $\Delta E_{NC}/2e$, there is net injection of electrons only into the two crossing subbands. When the applied voltage is larger than $\Delta E_{NC}/2e$, electrons are injected into the noncrossing subbands. The electrons injected into the noncrossing subbands can in principle contribute to the current only if final states into which they can be transmitted are available. As can be seen from Fig. 1, when $V_a \geqslant \Delta E_{NC}/e$, electrons incident into the first noncrossing subband below the band center (in the left contact) can tunnel into states of the first noncrossing subband above the band center (in the right contact). $\Delta E_{NC}/e$ is the equivalent of the barrier height for this tunneling process.

(ii) The length over which an applied bias drops. This corresponds to the barrier length [the distance across which an electron should tunnel to reach a right moving state (Fig. 1)] for electrons injected into the first noncrossing subband.

As ΔE_{NC} varies with diameter, we consider nanotubes with diameters varying from 6.8 to 27.2 Å. They are the (5,5) [3.64 eV], (10,10) [1.92 eV], (13,13) [1.48 eV], (16,16) [1.22 eV] and (20,20) [0.98 eV] nanotubes (ΔE_{NC} is given in the square brackets). The barrier length (and so the electric field) is varied by considering the potential to drop linearly in sections that are 10, 30, and 60 Å long. We have also calculated the effect of Zener tunneling by taking the applied potential (V_a) to drop across the nanotube as,

$$V(x) = \frac{V_a}{2}\left\{1 + \frac{1+e^{L_t/L_{sc}}}{e^{L_t/L_{sc}} - e^{-L_t/L_{sc}}} e^{-x/L_{sc}} - \frac{1+e^{-L_t/L_{sc}}}{e^{L_t/L_{sc}} - e^{-L_t/L_{sc}}} e^{x/L_{sc}}\right\}, \tag{3}$$

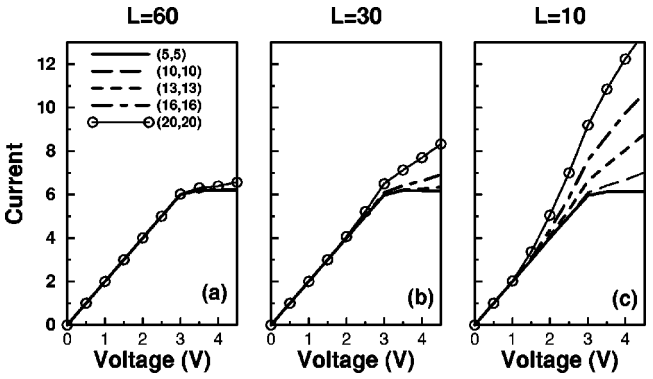

FIG. 2. Current versus applied voltage for three different lengths across which the applied voltage drops, (a) 60 Å, (b) 30 Å, and (b) 10 Å. The results for tubes with five different diameters are shown. Zener tunneling is negligible in (a). For a given nanotube, the importance of Zener tunneling increases with an increase in the electric field strength, as in (b) and (c). For a given applied voltage, the importance of Zener tunneling increases with an increase in nanotube diameter.

where L_t is the length of the nanotube, and a typical value of $L_t = 2500$ Å. L_{sc} is a parameter that determines the nature of the voltage drop and x is the nanotube axis. $L_{sc} > L$ corresponds to a linear voltage drop. $L_{sc} < L$ corresponds to a scenario with large potential drops near the left and right ends, and a flat potential in between. As a result, for an applied voltage, the maximum electric field is smaller when Eq. (3) is used instead of a linear potential drop. With the potential profile in Eq. (3), while there is a change in the form of transmission versus energy, the essential physics remains unchanged.

The results for the 60 Å case is discussed first. At applied voltages smaller than $\Delta E_{NC}/2e$, there is net injection of electrons only into the two crossing subbands. As a result, the I-V curve is linear, with the differential conductance equal to $4e^2/h$ (Fig. 2). This is true more or less independent of the distance over which the voltage drops. For $V_a > \Delta E_{NC}/2e$, electrons are injected into the higher subbands. Yet the maximum differential conductance in Fig. 2(a) is approximately $4e^2/h$. This is because electrons injected in the noncrossing subbands are primarily reflected, and so do not carry an appreciable current. To see this more clearly, consider the case of $V_a = 2.5$ V, where electrons are injected from the left into twenty subbands. In Fig. 3, we show that for the 60 Å case, all noncrossing subbands (solid and dotted lines) are almost fully Bragg reflected, and the crossing subbands are fully transmitted. Hence, the maximum differential conductance in Fig. 2(a) is approximately equal to $4e^2/h$. Alternately, electrons incident in the *noncrossing* subbands have to traverse a spatial region with only the *crossing* subbands, before tunneling into the right contact. Hence, in the absence of significant intersubband tunneling, they are reflected. The above picture changes at voltages above 3.1 V, which corresponds to a subband extrema of the crossing subbands. When $V_a > 3.1$ V, there is almost no increase in current with applied voltage, in the voltage regime considered. This regime is explained by using a (20,20) nanotube at $V_a = 3.5$ V (Fig. 4). When $V_a = 3.5$ V, electrons are injected into thirty-five subbands from the left contact at $E = -V_a$. However, in a small energy range near

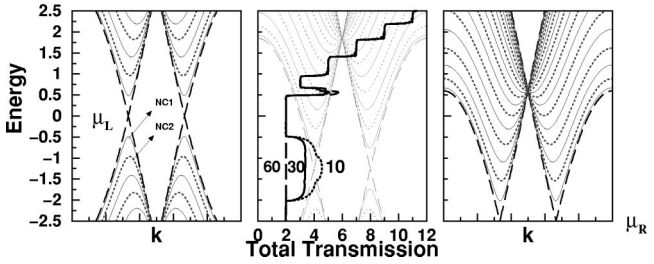

FIG. 3. The left and right columns are the nanotube band structure close to the left and right contacts, respectively. The central column is the total transmission versus energy for three different lengths (60, 30, and 10 Å) over which the voltage drops. The current (Fig. 2) is the integral of the total transmission from μ_R to μ_L. The Zener tunneling probability is negligible for the noncrossing subbands in the case of $L=60$ Å. For $L=30$ and 10 Å, the opening and closing of a transmission window due to the first noncrossing subband (solid line marked NC1) is seen. For $L=10$ Å, the opening and closing of a transmission window due to the second noncrossing subband (dotted line marked NC2) is also seen. $V_a=2.5$ V.

$E=0$ and $-V_a$, the total transmission is approximately one. This is because electrons injected into one of the two crossing subbands near $E=0$ are Bragg reflected (at $E=0$, only one of the two crossing subbands has a right moving state in the right contact). Similarly, near $E=\mu_L$, only one crossing subband has a right moving state at the left contact. In between these energy windows with unity total transmission, both crossing subbands are transmitted. The electrons injected into the noncrossing subbands are almost fully Bragg reflected, as discussed in the case of $V_a=2.5$ V. Upon increasing the applied voltage, the energy ranges where a single crossing subband carries current broadens, and the central energy range in between where both crossing subbands carry current (Fig. 3) becomes narrower. The current, which is approximately the integral of the area under the curve between $E=0$ and $-V_a$ does not increase much with further applied voltage, as shown in Fig. 2. The explanation for the other nanotubes in Fig. 2(a) is no different except that the larger value of the barrier height ΔE_{NC} makes Bragg reflection only more important when compared to the (20,20) nanotube.

The I-V characteristics in Fig. 2(a) are primarily determined by the crossing subbands because all other subbands

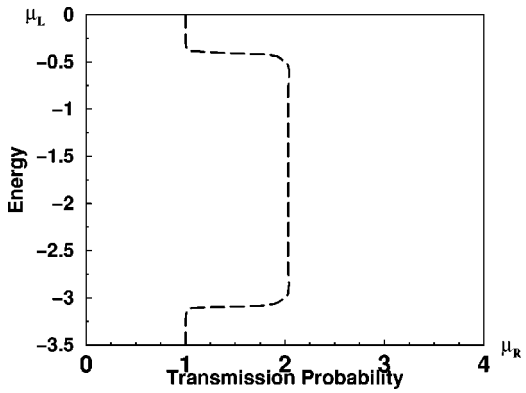

FIG. 4. The total transmission versus energy for $V_a=3.5$ V. The total transmission is equal to one in energy ranges near the band centers in the left and right contacts, where crossing subbands are absent at either the left or right ends. The total transmission in between is approximately two, corresponding to the transmission of both crossing subbands.

are almost completely Bragg reflected. This picture changes when intersubband Zener tunneling or defect induced intersubband scattering are non-negligible. To elucidate their effect on the I-V curve, we study their effects independently.

Zener tunneling, in principle, begins to occur when $V_a=\Delta E_{NC}/e$ (Fig. 1). At this voltage, electrons incident in the first noncrossing subband below $E=0$ (in the left contact) are able to tunnel into states of the first noncrossing subband above $E=0$ (in the right contact), as shown in Fig. 1. $\Delta E_{NC}/e$, which is the barrier height, decreases inversely with an increase in nanotube diameter [the diameter is directly proportional to N for a (N,N) nanotube], $\Delta E_{NC} \propto 1/N$ [Eq. (1)]. So, we expect Zener tunneling to become more important with an increase in nanotube diameter. Figures 2(b) and 2(c) show that the calculated I-V deviates significantly from Fig. 2(a) as a result of intersubband Zener tunneling. The main points are that Zener tunneling and hence deviation of current from Fig. 2(a) increases, (i) at smaller applied voltages, as the nanotube diameter increases and the corresponding barrier height decreases [Figs. 2(b) and 2(c)], and (ii) with increasing electric field [Figs. 2(a)–2(c)] as the distance over which an electron has to tunnel is smaller. A plot of the total transmission versus energy throws further light on the physics involved. When the bias drops over 30 Å, the opening and closing of a transmission window due to the first noncrossing subband (solid line marked NC1) is at energies of about 0.5 and 2.0 eV, respectively. These energies correspond to $\Delta E_{NC}/2$ below (0.5 eV) and above (2.0 eV) the nanotube band centers near the left and right contacts, respectively. In the case of $L=10$ Å, the opening and closing of a second transmission window due to the second noncrossing subband (dotted line marked NC2) at energies of about 1 and 1.5 eV, respectively, is seen. Also, the transmission probability of NC1 is larger in comparison to the 30 Å case because of the smaller barrier length. While the differential conductance at $V_a=2.5$ V is not comparable to the twenty injected subbands, the contribution to current due to Zener tunneling cannot be neglected.

Frank *et. al.* reported a constant conductance for applied voltages smaller than an estimate of $\Delta E_{NC}/e$ for their large diameter nanotubes, and a modest increase in conductance with applied bias for larger applied voltages.[4] This increase in conductance did not reflect the large increase in the number of subbands with bias. The transport bottleneck discussed in this paper offers a possible physical mechanism that qualitatively explains the small increase in conductance with applied voltage in Ref. 4.

Finally, we discuss the role of defect assisted intersubband scattering. From a physical viewpoint, Bragg reflection is weakened because defect scattering produces a nonzero probability for an electron incident in a noncrossing subband to reach the right contact, by scattering into right moving states of other subbands. To model defects, we follow section III A of Ref. 8, where the on-site potential is varied randomly. We consider a 2500 Å long nanotube section with defects, and the applied voltage drops linearly. So, Zener tunneling is not important here, and all intersubband tunneling is defect induced. The I-V curve is shown for two different strengths of defect scattering in Fig. 5. The numbers in the legend correspond to ϵ_{random} of Ref. 8, of which a larger value corresponds to larger defect scattering. In Fig. 5, at small

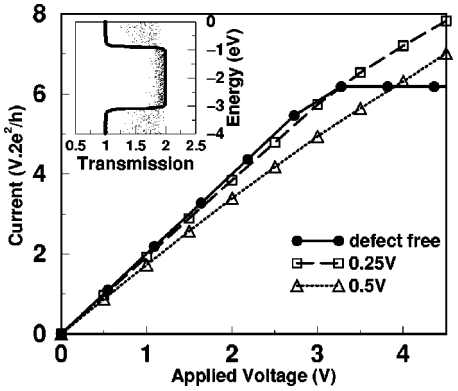

FIG. 5. Current versus applied voltage for a (10,10) nanotube in the presence of defects. For $V_a<3.1$ V, the differential conductance decreases with increase in the defect scattering strength. For $V_a>3.1$ V the differential conductance with defects is larger than the defect-free case. This is because intersubband scattering opens channels for transport involving the noncrossing subbands. The strength of defect scattering increases with an increase in ϵ_{random}. Inset: Total transmission versus energy with and without defect scattering, when $V_a=4$ V. Note that in comparison to the defect-free case, the total transmission is larger than one in energy windows near 0 and $-V_a$.

voltages, only the crossing subbands determine the physics. Hence, the reflection of electrons in the crossing subbands causes a diminished current and differential conductance in comparison to the defect-free case. At higher applied voltages, the differential conductance is larger than in the defect-free case because the noncrossing subbands are partially transmitted. Transmission of electrons incident in the noncrossing subbands is illustrated in the inset of Fig. 5, which is a plot of total transmission versus energy with and without defect scattering ($\epsilon_{random}=0.25$ eV) at $V_a=4$ V, for $-V_a<E<0$. Defect scattering enhances the total transmission near $E=0$ and $-V_a$ to values larger than in the defect-free case. Thus, showing that electrons injected in the crossing subbands are transmitted in noncrossing subbands at the right end (inset of Fig. 5).

While both Zener tunneling and defect scattering enhance the differential conductance at large applied voltages, the following features differentiate them. At biases smaller than $\Delta E_{NC}/e$, defects cause a reduction in current in comparison to the Zener tunneling case, which continues to yield a conductance of $4e^2/h$. At biases larger than $\Delta E_{NC}/e$, electrons are injected into many subbands. The differential conductance in the case of Zener tunneling is larger than $4e^2/h$. Defect scattering alone, on the other hand, produces a differential conductance that is smaller than $4e^2/h$. This is because electrons incident in the *noncrossing* subbands have to traverse a spatial region where only the *crossing* subbands are present, before being transmitted to the right contact.

In conclusion, we have investigated the current carrying capacity of carbon nanotubes by including transport through noncrossing subbands. This study considered ballistic transport and neglected electron-phonon interaction.[9] We showed that due to the unique band structure of carbon nanotubes, Bragg reflection of electrons incident in the noncrossing subbands is an important mechanism for the reduction of differential conductance. The differential conductance of nanotubes will be diameter dependent from purely ballistic processes due to competition between Bragg reflection and Zener-type intersubband tunneling. The importance of Zener tunneling was studied by varying both the nanotube diameter and the length over which the voltage drops. The barrier height for Zener tunneling is equal to the intersubband energy level spacing ΔE_{NC} of Fig. 1, which decreases inversely with an increase in nanotube diameter. As a consequence, for small diameter nanotubes, the differential conductance cannot be larger than $4e^2/h$ for voltages smaller than 3.1 V, and is close to zero at larger applied voltages. Zener tunneling becomes more important with increasing nanotube diameter because $\Delta E_{NC}\propto$ 1/Diameter. Also, Zener tunneling is stronger when the voltage drops across a smaller length. We show that, for increasing nanotube diameter, the noncrossing subbands carry current in certain energy windows (Fig. 3). As a result, the differential conductance at biases larger than $\Delta E_{NC}/e$ is larger than $4e^2/h$ (Fig. 2). It should be emphasized that the differential conductance is, however, not comparable to the large number of subbands into which electrons are injected from the contacts. The role of defect scattering in the absence of Zener tunneling is also discussed. It is shown that at biases smaller than 3.1 V, defect scattering leads to a differential conductance that is smaller than $4e^2/h$. For biases larger than 3.1 V, defects increase the differential conductance when compared to the defect-free case.

Useful discussions with Zhen Yao, Cees Dekker, T. R. Govindan, Adrian Batchold, and Walt de Heer are acknowledged. I would like to thank Bryan Biegel for correcting an earlier version of the manuscript and discussions.

[1] S. J. Tans, M. Devoret, H. Dai, A. Thess, R. E. Smalley, L. J. Geerligs, and C. Dekker, Nature (London) **386**, 474 (1997).

[2] D. H. Cobden, M. Bockrath, P. L. McEuen, A. G. Rinzler, and R. E. Smalley, Phys. Rev. Lett. **81**, 681 (1998).

[3] H. T. Soh, C. F. Quate, A. P. Morpurgo, C. M. Marcus, J. Kong, and H. Dai, Appl. Phys. Lett. **75**, 627 (1999).

[4] S. Frank, P. Poncharal, Z. L. Wang, and W. A. de Heer, Science **280**, 1744 (1998); P. Poncharal, S. Frank, Z. L. Wang, and W. A. de Heer (unpublished).

[5] C. Schonenberger, A. Bachtold, C. Strunk, J.-P. Salvetat, and L. Forro, Appl. Phys. A: Mater. Sci. Process. **A69**, 283 (1999).

[6] P. J. de Pablo, E. Graugnard, B. Walsh, R. P. Andres, S. Datta, and R. Reifenberger, Appl. Phys. Lett. **74**, 323 (1999).

[7] M. F. Lin and D. S. Chuu, Phys. Rev. B **56**, 4996 (1997).

[8] M. P. Anantram and T. R. Govindan, Phys. Rev. B **58**, 4882 (1998); M. P. Anantram, Jie Han, and T. R. Govindan, Ann. (N.Y.) Acad. Sci. **852**, 169 (1998).

[9] Z. Yao, C. L. Kane, and C. Dekker, Phys. Rev. Lett. **84**, 2941 (2000).